

Phase diagram and electrostrictive properties of $\text{Bi}_{0.5}\text{Na}_{0.5}\text{TiO}_3\text{-BaTiO}_3\text{-K}_{0.5}\text{Na}_{0.5}\text{NbO}_3$ ceramics

Shan-Tao Zhang,^{1,2} Feng Yan,^{2,a)} Bin Yang,³ and Wenwu Cao⁴

¹Department of Materials Science and Engineering and National Laboratory of Solid State Microstructures, Nanjing University, Nanjing 210093, People's Republic of China

²Department of Applied Physics, The Hong Kong Polytechnic University, Hung Hom, Kowloon, Hong Kong

³Department of Physics, Center for Condensed Matter Science and Technology, Harbin Institute of Technology, Harbin 150001, People's Republic of China

⁴Materials Research Institute, The Pennsylvania State University, University Park, Pennsylvania 16802, USA

(Received 14 April 2010; accepted 2 September 2010; published online 23 September 2010)

Phase diagram of $\text{Bi}_{0.5}\text{Na}_{0.5}\text{TiO}_3\text{-BaTiO}_3\text{-K}_{0.5}\text{Na}_{0.5}\text{NbO}_3$ ternary system has been analyzed and $(0.94-x)\text{BNT}-0.06\text{BT}-x\text{KNN}$ ($0.15 \leq x \leq 0.30$) ceramics have been prepared and investigated. Pseudocubic structures were confirmed by x-ray diffractions and its preliminary Rietveld refinements. P-E, S-E, and S-P² profiles (where P, E, and S denote polarization, electric field, and strain, respectively) indicate electrostrictive behavior of all ceramics. The compositions with $x = 0.20$ and 0.25 show pure electrostrictive characteristics. The dissipation energy, electrostrictive strain, and electrostrictive coefficient have been determined and compared with other lead-free and lead-containing electrostrictors. The electrostrictive coefficient can reach as high as $0.026 \text{ m}^4/\text{C}^2$, about 1.5 times of the value of traditional Pb-based electrostrictors. © 2010 American Institute of Physics. [doi:10.1063/1.3491839]

Both electrostrictive and piezoelectric ceramics are commercially used in electromechanical devices, such as actuators, space mirrors, etc. Electrostrictors have special advantages over piezoelectrics, because they do not require poling process and there is negligible hysteresis in strain-electric field (S-E) cycle, which is important for precision position control.¹⁻³ In electrostriction, the sign of the field-induced deformation is independent of the polarity of the field and is proportional to the square of the applied electric field

$$S = QP^2, \quad (1)$$

where Q is the electrostrictive coefficient and P is polarization.²

In recent years, a lot of attention has been paid to lead-free piezoelectric materials^{4,5} but much less effort was devoted to high-performance lead-free electrostrictors.⁶⁻⁹ One of the reasons might be due to the much smaller commercial market for high performance electrostrictors than for piezoelectric devices. Another reason might be due to the lack of public awareness on the fact that most of currently used electrostrictors are also lead based materials. With increasing pressure from environmental legislations, lead-free piezoelectric and electrostrictive materials are urgently in demand. Therefore, it is just as important to study lead-free electrostrictive materials as lead-free piezoelectric materials.

Electrostriction is a general property of all dielectric materials but it is significantly large in ferroelectrics just above the Curie temperature (T_c), where an electric field can induce energetically unstable ferroelectric phase. In relaxor ferroelectrics, the electrostrictive strain can be kept at a relatively high level in a wide temperature range, because of the diffused phase transition.² If the phase transition temperature of a relaxor ferroelectrics is close to room temperature (RT), the

electrostrictive effect can be very large at RT. Therefore, one may adjust the composition or dopants in lead-free relaxor ferroelectrics to produce pseudocubic/cubic crystal structure at RT, which might produce good lead-free electrostrictors. Recently reported electrostrictors, $(\text{Sr}_{1-y-x}\text{Na}_y\text{Bi}_x)\text{TiO}_3$ and $\text{Bi}_{0.5}\text{Na}_{0.5}\text{TiO}_3\text{-BaTiO}_3\text{-K}_{0.5}\text{Na}_{0.5}\text{NbO}_3$ (BNT-BT-KNN), have the above mentioned features of relaxor characteristics, such as paraelectric state and pseudocubic structure at RT,^{7,8} as evidenced by frequency dependent relative dielectric constant (ϵ_r) and dielectric loss ($\tan \delta$), x-ray diffraction (XRD) patterns, and almost linear polarization-electric field (P-E) profiles.

There is a ferroelectric-antiferroelectric phase transition in lead-free BNT-based ferroelectrics. Proper substitutions can help decrease the phase transition temperature to near RT, and enhance the relaxor behavior at RT.⁷⁻¹² In addition, BNT, BT, and KNN are typical end members for developing lead-free piezoelectric materials.⁴ Structure and piezoelectric property of their binary and ternary solid solutions have been widely studied.^{10,13-18} According to related reports, there are seven binary morphotropic phase boundaries (MPBs) constructed by BNT, BT, and KNN,¹³⁻¹⁸ as shown in Fig. 1. According to those reports, the compositions between MPB-3 and MPB-4, as well as between MPB-6 and MPB-7 have pseudocubic/cubic structure. In addition, MPB-1 composition without poling has pseudocubic/cubic structure.^{10,19} Accordingly, the compositions located in the center area of the phase diagram enclosed by the red lines might have pseudocubic/cubic structure near RT. It must be noted that Fig. 1 is only a schematic phase diagram of BNT-BT-KNN.

From structural consideration, the reported BNT- and BT-based electrostrictive materials, e.g., BNT-(Bi,Sr)TiO₃ and BaTiO₃-CaTiO₃, have pseudocubic structure at RT.^{6,7} Although no electrostrictive effect has been reported in KNN-based materials, pseudocubic KNN-SrTiO₃ shows

^{a)}Electronic mail: apafyan@polyu.edu.hk.

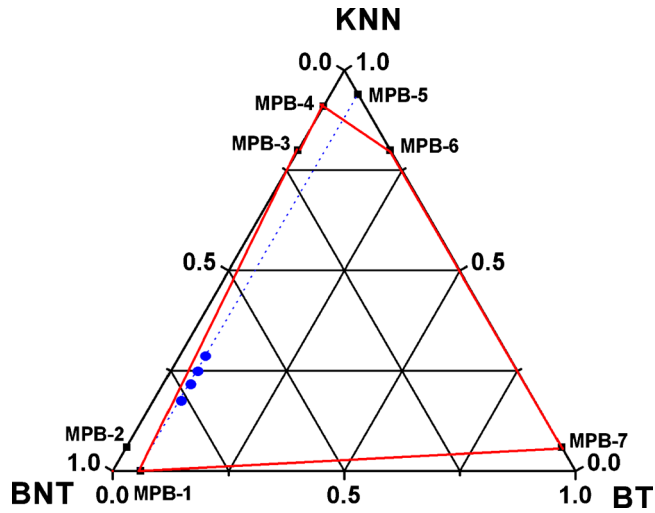


FIG. 1. (Color online) The phase diagram of BNT–BT–KNN ternary system. The MPB- n ($n=1-7$) corresponds to 0.94BNT–0.06BT, 0.94BNT–0.06KNN, 0.80KNN–0.20BNT, 0.091KNN–0.09BNT, 0.94KNN–0.06BT, 0.80KNN–0.20BT, and 0.94BT–0.06KNN, respectively. These MPBs separate rhombohedral-tetragonal, rhombohedral-tetragonal, tetragonal(rhombohedral)-cubic, cubic-orthorhombic, orthorhombic-tetragonal, tetragonal-cubic, and cubic-tetragonal, respectively (Refs. 13–18).

some indications of electrostrictive behavior.^{20,21} Counterparts of the above mentioned BNT-, BT-, and KNN-based electrostrictors with pseudocubic/cubic structure can be designed in the center pseudocubic/cubic area of the phase diagram shown in Fig. 1. In fact, a BNT–BT–KNN ternary compositions very close to the line connecting MPB-1 and MPB-3, have been confirmed experimentally to be pure electrostrictive.⁸

By further comparison, it is noticed that BT-rich electrostrictors generally show lower strain ($\sim 0.03\%$) than BNT-rich electrostrictors (~ 0.1).^{7,8} This suggests that BNT-rich BNT–BT–KNN ternary compounds with compositions located in the pseudocubic/cubic area may be good electrostrictors.

According to previous reports,¹⁰ $(0.94-x)\text{BNT}-0.06\text{BT}-x\text{KNN}$ with $x=0.12$, has slim P-E and S-E profiles, which indicated the possibility of developing BNT–BT–KNN based lead-free electrostrictor by further increasing the KNN content. In this paper, $(0.94-x)\text{BNT}-0.06\text{BT}-x\text{KNN}$ ceramics with $0.15 \leq x \leq 0.30$, located in the pseudocubic/cubic area, as indicated by the green dots in Fig. 1, were prepared and investigated. We found that these compounds are electrostrictive material with large electrostrictive coefficients.

The ceramics were prepared by solid state reaction method. Dried raw materials of Bi_2O_3 (99.8%), Na_2CO_3 (99.8%), TiO_2 (99.0%), BaCO_3 (99.0%), K_2CO_3 (99.0%), and Nb_2O_5 (99.6%) were mixed according to the stoichiometric formula and ball milled for 24 h in ethanol. The dried slurries were calcined at 900°C for 3 h and then ball milled again for 24 h. The powders were subsequently pressed into green disks with a diameter of 10 mm under 60 MPa pressure. Sintering was carried out in covered alumina crucibles at 1100°C . To reduce the volatility of Bi, Na, and K during firing, the disks were embedded in the powder. The crystal structure of the ceramics was characterized by powder XRD (Rigaku Ultima III). The circular surfaces of the disks were

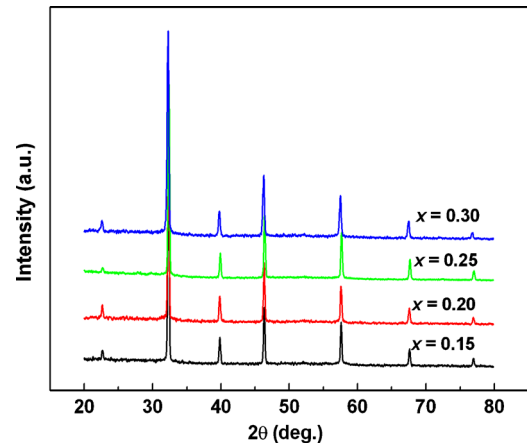


FIG. 2. (Color online) XRD pattern of the ceramics.

covered with a thin layer of silver paste and fired at 550°C for 30 min for electrical measurements. Relative dielectric constant (ϵ_r) and loss tangent ($\tan \delta$) of unpoled ceramics were measured using an impedance analyzer (HP4294A) at frequencies from 100 Hz to 1 MHz in the temperature range from 50 to 400°C . Both polarization-electric field (P-E) and strain-electric field (S-E) curves were measured at 1 Hz by precision premier II (Radiant Tech. USA) at RT in silicone oil.

Figure 2 plots typical XRD patterns of the ceramics. All peaks can be indexed by perovskite structure, indicating the formation of single phase ceramics and the sharp peaks indicate that the ceramics are well crystallized. No peak splitting was detected in all patterns and our preliminary Rietveld simulation on the composition with $x=0.30$ revealed that the ceramics have a pseudocubic structure. This is consistent with previous Rietveld simulations based on high resolution XRD for $(0.94-x)\text{BNT}-0.06\text{BT}-x\text{KNN}$ with $0 \leq x \leq 0.11$.^{10,19}

The measured P-E and S-E profiles are shown in Fig. 3. The slightly nonlinear P-E profiles at the fields of 8 kV/mm are slimmer than that of other lead-free or lead-containing electrostrictors.^{7,8} In addition, the dissipated energy, i.e., the area of the P-E curves, are determined to be

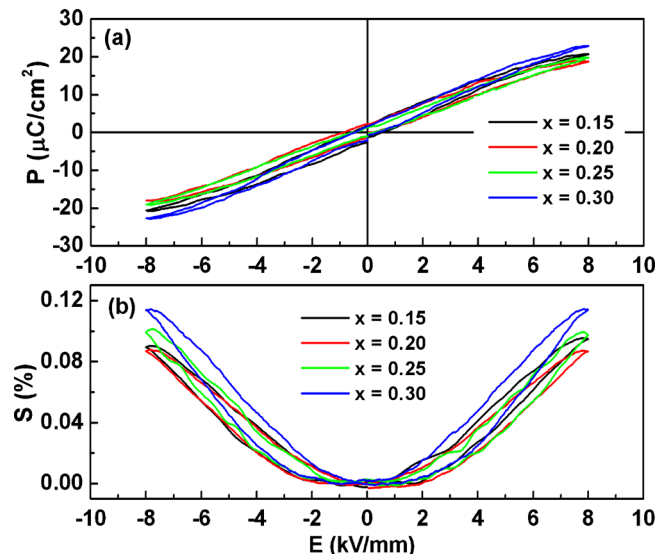


FIG. 3. (Color online) (a) P-E and (b) bipolar S-E curves of the ceramics.

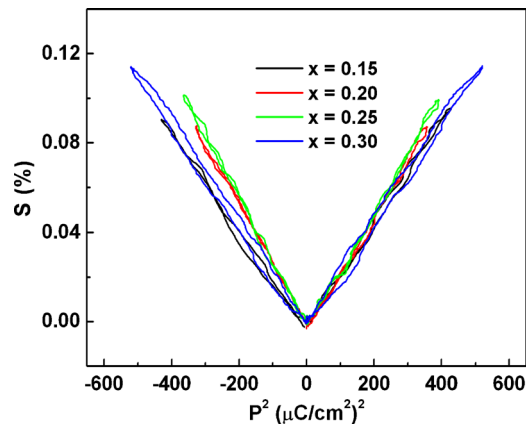


FIG. 4. (Color online) S - P^2 curves of the ceramics, indicating electrostrictive effect.

0.21×10^6 J/m³, 0.17×10^6 J/m³, 0.15×10^6 J/m³, and 0.20×10^6 J/m³, respectively. These values are lower than that of other reported electrostrictive materials.⁸ On the other hand, the S - E curves show very little hysteresis with strain value in the range of 0.09%–0.11%. This strain level is comparable with other lead-containing electrostrictors.^{7,8,22}

Shown in Fig. 4 are the plots of S versus P^2 . Clearly, the S - P^2 curves for the composition with $x=0.20$ and 0.25 are linear whereas that of $x=0.15$ and 0.30 are slightly deviated from liner relations. That means the composition with $x=0.20$ and 0.25 are pure electrostrictors whereas with $x=0.15$ and 0.30 show predominant electrostrictive behavior. The averaged electrostrictive coefficient (Q) is calculated to be 0.021, 0.026, 0.025, and 0.022 m⁴/C² for the compositions with $x=0.15$, 0.20, 0.25, 0.30, respectively. We note that the Q value of lead-based electrostrictive material, such as Pb(Mg,Nb)O₃–PbTiO₃, is reported to be about 0.017.²³ That means the Q values of our materials are notably larger than that of lead-based electrostrictors.^{7,8}

The dielectric constant ϵ_r and loss $\tan \delta$ of the composition $x=0.30$ were measured at different frequencies as a

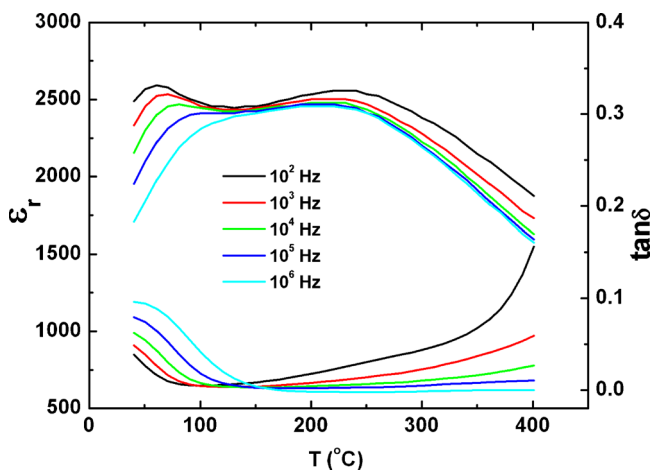


FIG. 5. (Color online) Temperature dependence of ϵ_r and $\tan \delta$ of the composition with $x=0.30$, other compositions show similar dielectric properties.

function of temperature as shown in Fig. 5. The frequency dependent ϵ_r and $\tan \delta$ near RT show typical relaxor characteristics. In addition, the dielectric constant ϵ_r versus temperature curve is rather flat, with variation less than $\pm 10\%$ in the temperature range between 40 and 250 °C at low frequencies. Other compositions show very similar temperature dependent dielectric properties.

In conclusion, phase diagram of BNT–BT–KNN ternary system has been analyzed. Regions with pseudocubic/cubic crystal structure in the ternary phase diagram were predicted to be electrostrictors, which was experimentally confirmed. Pseudocubic (0.94– x)BNT–0.06BT– x KNN with $0.15 \leq x \leq 0.30$ ceramic samples have been prepared and characterized. Electrostrictive effects have been observed in all samples and the $x=0.20$ and 0.25 compositions show pure electrostrictive behavior with low dissipated energy, high electrostrictive strain, and high electrostrictive coefficient. Our results are helpful for further investigation on high performance lead-free electrostrictors.

This work was supported by the Hong Kong Polytechnic University (Grant No. A-PH92), National Nature Science Foundation of China (Grant Nos. 10874069 and 10704021), the New Century Excellent Talents in University (Grant No. NCET-08-0279), and Natural Scientific Research Innovation Foundation in Harbin Institute of Technology (Grant No. HIT.NSRIF 201055).

¹S.-E. Park and T. R. Shrout, *J. Appl. Phys.* **82**, 1804 (1997).

²G. H. Haertling, *J. Am. Ceram. Soc.* **82**, 797 (1999).

³J. Rödel, W. Jo, K. T. P. Serfert, E.-M. Anton, and T. Granzow, *J. Am. Ceram. Soc.* **92**, 1153 (2009).

⁴S. J. Zhang, R. Xia, and T. R. Shrout, *J. Electroceramics* **19**, 251 (2007).

⁵Y. Saito, H. Takao, T. Tani, T. Nonoyama, K. Takator, T. Homma, T. Nagaya, and M. Nakamura, *Nature (London)* **432**, 84 (2004).

⁶X. Wang, H. Yamada, and C.-N. Xu, *Appl. Phys. Lett.* **86**, 022905 (2005).

⁷C. Ang and Z. Yu, *Adv. Mater.* **18**, 103 (2006).

⁸S. T. Zhang, A. B. Kounga, W. Jo, C. Jamin, K. Seifert, T. Granzow, J. Rödel, and D. Damjanovic, *Adv. Mater.* **21**, 4716 (2009).

⁹C. Ang and Z. Yu, *Appl. Phys. Lett.* **95**, 232908 (2009).

¹⁰S. T. Zhang, A. B. Kounga, E. Aulbach, H. Ehrenberg, and J. Rödel, *Appl. Phys. Lett.* **91**, 112906 (2007).

¹¹Y. Hiruma, Y. Imai, Y. Watanabe, H. Nagata, and T. Takenaka, *Appl. Phys. Lett.* **92**, 262904 (2008).

¹²Y. Hiruma, H. Nagata, and T. Takenaka, *J. Appl. Phys.* **104**, 124106 (2008).

¹³T. Takenaka, K. Maruyama, and K. Sakata, *Jpn. J. Appl. Phys., Part 1* **30**, 2236 (1991).

¹⁴A. B. Kounga, S. T. Zhang, W. Jo, T. Granzow, and J. Rödel, *Appl. Phys. Lett.* **92**, 222902 (2008).

¹⁵R. Z. Zuo, X. S. Fang, and C. Ye, *Appl. Phys. Lett.* **90**, 092904 (2007).

¹⁶C.-H. Choi, C.-W. Ahn, S. Nahm, J.-O. Hong, and J.-S. Lee, *Appl. Phys. Lett.* **90**, 132905 (2007).

¹⁷Y. P. Guo, K.-I. Kakimoto, and H. Ohsato, *Jpn. J. Appl. Phys., Part 1* **43**, 6662 (2004).

¹⁸R. P. Wang, H. Bando, and M. Itoh, *Appl. Phys. Lett.* **95**, 092905 (2009).

¹⁹J. E. Daniels, W. Jo, J. Rödel, and J. L. Jones, *Appl. Phys. Lett.* **95**, 032904 (2009).

²⁰V. Bobnar, J. Bernard, and M. Kosec, *Appl. Phys. Lett.* **85**, 994 (2004).

²¹M. Kosec, V. Bobnar, M. Hrovat, J. Bernard, B. Malic, and J. Holc, *J. Mater. Res.* **19**, 1849 (2004).

²²W. H. Jiang and W. W. Cao, *Appl. Phys. Lett.* **77**, 1387 (2000).

²³A. Furuta and K. Uchino, *J. Am. Ceram. Soc.* **76**, 1615 (1993).